IEEE Access
Multidisciplinary : Rapid Review : Open Access Journal

Received March 11, 2019, accepted March 26, 2019, date of publication March 29, 2019, date of current version April 12, 2019.

Digital Object Identifier 10.1109/ACCESS.2019.2908205

Autonomous Flight Control for Multi-Rotor UAVs Flying at Low Altitude

YUQING CHEN[1], GAOXIANG ZHANG[1], YAN ZHUANG[2], (Member, IEEE), AND HUOSHENG HU[3], (Senior Member, IEEE)

[1]School of Marine Electrical Engineering, Dalian Maritime University, Dalian 116026, China
[2]School of Control Science and Engineering, Dalian University of Technology, Dalian 116024, China
[3]School of Computer Science and Electronic Engineering, University of Essex, Colchester CO4 3SQ, U.K.

Corresponding author: Yan Zhuang (zhuang@dlut.edu.cn)

This work was supported in part by the Fundamental Research Funds for the Central Universities of China under Grant 3132016311, and in part by the Natural Science Foundation of Liaoning Province under Grant 20180520036.

ABSTRACT Unmanned aerial vehicles (UAVs) at low altitude flight may significantly degrade their performance and the safety under wind disturbances and incorrect operations. This paper presents a robust control strategy for UAVs to achieve good performance of low altitude flight and disturbance rejection. First, a novel second-order hexacopter dynamics is established and the position tracking is translated to the altitude and the rotational angle tracking problem. An integrated control scheme is created to deal with the challenges faced by hexacopter at low altitude flight, in which the influence of near-ground threshold distance and the desired roll, pitch, and yaw are analyzed. Moreover, an improved flying altitude planner and an attitude planner for low altitude conditions are designed respectively to avoid the overturning risk due to the big reaction torque and external disturbances. Second, a sliding-mode-based altitude tracking controller and an attitude tracking controller are designed to reduce the tracking errors and improve the robustness of the system. Finally, the proposed control scheme is tested on simulation and experiment platforms of multi-rotor UAV to show the feasibility and accurate trajectory tracking at low altitude flight.

INDEX TERMS Modeling, tracking control, low altitude, hexacopter, robustness.

I. INTRODUCTION

Currently, Unmanned Aerial Vehicles (UAVs) are very popular and widely used in scientific research and real-world applications such as remote sensing and air transportation. Many kinds of UAVs with six or more rotors have been developed and deployed in industrial fields due to their easy operation and increased total payload [1]–[3]. However, their successful deployments in the real world require a high degree of flight safety and robust trajectory tracking [4]. Especially, UAVs at low altitude flight are prone to fatal accidents due to unpredictable disturbances and misoperations. Therefore, it is necessary to develop an effective control strategy for UAVs to avoid overturning in the near-ground flight and ensure their safety operations, as well as the safety of public life and property [5].

To solve these problems, many automatic control methods have been proposed in literatures, including model predictive control [6], linear quadratic regulator [7], proportional integral derivative control [8], fuzzy control [9], [10], back stepping control [11], sliding mode control and adaptive control [12]–[14]. It became clear that attenuation control strategies and disturbance observer can effectively eliminate the influence of external disturbances and model uncertainties to ensure good attitude tracking performance [15]–[17]. Fuzzy neural networks were used for the trajectory tracking of UAV in [18] and shown that the optimal tuning algorithm is superior to the conventional PD controller in terms of tracking accuracy but requires more control effort.

In addition, sliding mode control is well known for its robustness in dynamic and complex environments, mainly due to its inherent ability to reject uncertainties and eliminate external disturbances. Therefore, it is widely used in to various UAVs [19]–[21], except for the case of so-called chattering phenomenon. Most of the existing research work has been focused on system modeling and attitude control algorithms for multi-rotor UAVs [22]–[28], The influence of misoperations and disturbances on the flight safety of UAVs

The associate editor coordinating the review of this manuscript and approving it for publication was Yue Zhang.

2169-3536 © 2019 IEEE. Translations and content mining are permitted for academic research only.
Personal use is also permitted, but republication/redistribution requires IEEE permission.
See http://www.ieee.org/publications_standards/publications/rights/index.html for more information.

has not been well investigated. Automatic attitude controllers with capabilities of misoperation prevention and disturbance rejection are much in demand to ensure flight safety for UAVs at the near-ground flight.

In the practical operation process of near-ground flight, UAVs normally encounter the following challenges: (i). Large cross-wind disturbances may cause an UAV to move away from the desired trajectory or overturn as it has a high gravity center; (ii). When an UAV is inclined to take off and landing and its bottom bracket contacts with the ground, the center of gravity of its body is offset and capsized. The UAV will collide with the ground under the action of lateral driving force and inertia force; (iii). When the UAV is operated manually near the ground, any wrong operation may give UAV a larger lateral driving torque, leading to the overturn of the fuselage. These accidents could break the wing or damage the electrical parts, antenna and other units. Therefore, it is very critical to develop a high-performance control system to enhance the attitude control stability of UAVs at low altitude flight.

This paper presents a robust control strategy for UAVs to achieve good performance of low attitude flight and disturbance rejection. More specifically, robust sliding mode-based controllers are deployed to increase the overall efficiency of hexacopter operation. The main focus of this work is to implement a robust control system for a hexacopter to realize attitude adjustment and disturbance rejection at low attitude flight. Nonlinear dynamics of hexacopter is studied, and low altitude planners are proposed by increasing the altitude to avoid collision and overturning if attitude angles are too big. The closed-loop system stability is ensured for a selected maximum admissible value of the external disturbances. The main contribution of this work is threefold:

(1) Express the hexacopter dynamics as a novel second-order equations of position and attitude, and then translate the tracking position to a quaternion which includes the altitude and the rotational angles.
(2) An integrated control scheme is proposed for the low altitude flight of hexacopter from a practical perspective. Consider the flying states, an improved flying attitude close-to-ground planner (ATCGP) and an altitude close-to-ground planner (ALCGP) are designed to avoid the overturning risk due to the big roll and pitch angles from misoperations or external disturbances.
(3) Robust tracking controllers are created for effectively handling disturbance to achieve precise trajectory tracking. To reduce the tracking error and improve the robustness of the system, sliding-mode control method is used in the design of the altitude tracking controller and attitude tracking controller respectively.

The rest of this paper is organized as follows. Section II presents the dynamic differential equations of hexacopter and the construction of the hexacopter model. Section III proposes a system control scheme that includes the tracking controllers and some effective control strategies for low altitude flight and avoiding overturning with proper planners. In Section IV, the main procedures of position tracking controllers are presented for effectively handling disturbances existed in a hexacopter to achieve highly precise trajectory tracking. Then, the proposed control scheme is tested on simulation and experimental UAVs with 6 rotors in Section V. Autonomous take-off and landing cases and low-altitude control techniques without collision are discussed. The results of numeric tests are given to show the feasibility and performance of the proposed approach. Finally, a brief conclusion and future work are given in Section VI.

II. MODELING AND DYNAMICS

A. DYNAMICS OF HEXACOPTER

In this section, the dynamic differential equations of the hexacopter are established that is considered as a rigid frame attached with six rotors, and the center of gravity coincides with the body-fixed frame origin. Rotors R_1, R_3 and R_5 rotate counterclockwise, and the rotors R_2, R_4 and R_6 rotate clockwise. Each propeller rotates at the angular velocity ω_i. Therefore, a force F_i is produced along the z-direction relative to the body frame and a reaction torque M_i is generated on the hexacopter body by each rotor as:

$$\begin{cases} F_i = k_T \omega_i^2, \\ M_i = (-1)^{i+1} k_Q \omega_i^2. \end{cases} \qquad i = 1, 2, \cdots, 6 \tag{1}$$

where $k_T = c_T \rho r^4 \pi > 0$ denotes the aerodynamic coefficient, which is obtained by multiplying the atmospheric density ρ, the radius of the propeller r, and the thrust coefficient c_T. In addition, $k_Q = c_Q \rho r^5 \pi > 0$ denotes the drag coefficient of the rotor, which also depends on ρ, r and the torque coefficient c_Q.

The variation of the orientation is achieved by varying the angular velocity of a specific rotor. The force and the torque created around a particular axis with respect to the body-fixed frame is defined as $u = [\,U_1\ U_2\ U_3\ U_4\,]^T$ which is the control signal to be designed and satisfies:

$$u = K[\,\omega_1^2 \quad \omega_2^2 \quad \omega_3^2 \quad \omega_4^2 \quad \omega_5^2 \quad \omega_6^2\,]^T \tag{2}$$

where K is a constant coefficient matrix and the components $U_{1\sim4}$ represent the total lift, roll, pitch and yaw moments of the hexacopter respectively.

NOTATION: Assume matrices $M \in \mathbb{R}^{m\times1}$ and $N \in \mathbb{R}^{m\times n}$, define a weighting operator Θ and the operation $M\Theta N$ denotes that the multiplication of each row element of matrix N by the corresponding row element of the first column vector M.

Under the above notation, the matrix K in (2) for a symmetrical rigid hexacopter can be expressed as:

$$K = \begin{bmatrix} k_T \\ k_T l \\ k_T l \\ k_Q \end{bmatrix} \Theta \begin{bmatrix} 1 & 1 & 1 & 1 & 1 & 1 \\ -1/2 & -1 & -1/2 & 1/2 & 1 & 1/2 \\ \sqrt{3}/2 & 0 & -\sqrt{3}/2 & -\sqrt{3}/2 & 0 & \sqrt{3}/2 \\ -1 & 1 & -1 & 1 & -1 & 1 \end{bmatrix}$$

where l is the length of each arm.

In the mathematical model of hexacopter shown in Figure 1, two coordinate frames are considered: the non-moving inertial frames $O_{\mathrm{E}}\{x_E, y_E, z_E\}$ and the body-fixed frame $O_{\mathrm{B}}\{x_B, y_B, z_B\}$ to represent the actual position and actual attitude of hexacopter respectively. Note that the NED coordinates are used to define all the frames. In this paper, the position of the hexacopter is written as $\xi = \begin{bmatrix} x & y & z \end{bmatrix}^T$ and the attitude angle of the hexacopter is denoted as $\eta = \begin{bmatrix} \phi & \theta & \psi \end{bmatrix}^T$ in the inertial frame O_{E}. The range of the attitude angle is $0 \leq \eta < \eta_L, \eta_L = \begin{bmatrix} \pi/2 & \pi/2 & 2\pi \end{bmatrix}^T$.

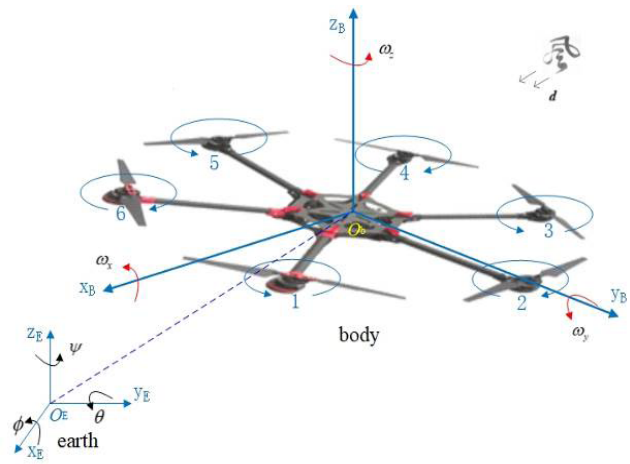

FIGURE 1. Hexacopter frames.

According to Newton's second law and theorem of moment of momentum, the translational and rotational dynamics of the hexacopter in frame O_{b} are summarized as:

$$\begin{aligned} F_b &= m\dot{v}_b + m\Omega \times v_b \\ M_b &= I\dot{\Omega} + \Omega \times I\Omega \end{aligned} \tag{3}$$

where m is the mass, F_{b} and M_{b} are resultant force and moment acting on the UAV in the frame O_{B}, and v_b denotes the linear velocity and $\Omega = \begin{bmatrix} \omega_x & \omega_y & \omega_z \end{bmatrix}^T$ denotes the angular velocity, and $\boldsymbol{I} = \mathrm{diag}[I_x, I_y, I_z]$ is the constant matrix of the moment of inertia around x-axis, y-axis and z-axis. Then we have:

$$\begin{cases} \dot{\xi} = (C_\phi C_\theta C_\psi)^T v_b \\ \dot{\Omega} = \dot{\phi} I_1 + C_\phi(\dot{\theta} I_2 + C_\theta(\dot{\psi} I_3)) \end{cases} \tag{4}$$

where C_ϕ, C_θ and C_ψ denote the rotation matrices in the angle ϕ, θ and ψ respectively, and $I_1 = \begin{bmatrix} 1 & 0 & 0 \end{bmatrix}^T$, $I_2 = \begin{bmatrix} 0 & 1 & 0 \end{bmatrix}^T$, $I_3 = \begin{bmatrix} 0 & 0 & 1 \end{bmatrix}^T$, and

$$C_\phi = \begin{bmatrix} 1 & 0 & 0 \\ 0 & c_\phi & s_\phi \\ 0 & -s_\phi & c_\phi \end{bmatrix}, C_\theta = \begin{bmatrix} c_\theta & 0 & -s_\theta \\ 0 & 1 & 0 \\ s_\theta & 0 & c_\theta \end{bmatrix},$$
$$C_\psi = \begin{bmatrix} c_\psi & s_\psi & 0 \\ -s_\psi & c_\psi & 0 \\ 0 & 0 & 1 \end{bmatrix}$$

where the matrix element $c_{\phi,\theta,\psi}$ and $s_{\phi,\theta,\psi}$ denote the triangle function $\cos(\cdot)$ and $\sin(\cdot)$ of the rotation angles respectively.

Differentiating (4), the final form of hexacopter dynamics are reconstructed by the second-order equations:

$$\ddot{\xi} = A_\xi(U_\xi + d_\xi) + B_\xi \tag{5}$$
$$\ddot{\eta} = A_\eta(U_\eta + d_\eta) \tag{6}$$

where $U_\xi = U_1$, $U_\eta = \begin{bmatrix} U_2 & U_3 & U_4 \end{bmatrix}^T$. $d_\xi = [0 \;\; 0 \;\; d_z]^{\mathrm{T}}$ and $d_\eta = [d_\phi \;\; d_\theta \;\; d_\psi]^{\mathrm{T}}$ are wind force disturbances. In above equations, the coefficient matrices are shown as:

$$A_\xi = \frac{1}{m}\begin{bmatrix} s_\phi s_\psi + c_\phi s_\theta c_\psi \\ -s_\phi c_\psi + c_\phi s_\theta s_\psi \\ c_\theta c_\phi \end{bmatrix}, \quad B_\xi = \begin{bmatrix} 0 & 0 & -g \end{bmatrix}^T,$$
$$A_\eta = \begin{bmatrix} c_\theta & c_\theta s_\phi & -c_\theta c_\phi \\ 0 & c_\theta c_\phi & -c_\theta s_\phi \\ 0 & s_\phi & c_\phi \end{bmatrix} \boldsymbol{I}$$

In practice, we can use GPS and inertial measurement unit (IMU) to measure the position information ξ and attitude information η.

B. PROBLEM FORMULATION

In the trajectory tracking of UAV, desired positions are taken as the target values of motion control. To study the transient and steady-state characteristics of hexacopter, we use $\xi_d = \begin{bmatrix} x_d & y_d & z_d \end{bmatrix}^T$ to denote the desired position, then:

$$\xi_e = \xi_d - \xi \quad \rightarrow \begin{cases} z_e = z_d - z \\ \eta_e = \eta_d - \eta \end{cases} \tag{7}$$

where $\xi_e = \begin{bmatrix} x_e & y_e & z_e \end{bmatrix}^T$ is the tracking position error. Furthermore, because the errors in x and y are coupled with the attitudes of multi-rotor UAVs, It is taken for granted that the position error is translated to the tracking altitude error z_e and the rotational angular error $\eta_e = \begin{bmatrix} \phi_e & \theta_e & \psi_e \end{bmatrix}^T$.

In Section 4.1, the altitude control in the position loop is obtained by using a sliding mode controller PL-SMC, and the lift solution of altitude control can be obtained by formula (5):

$$U_1 = f_z(z_e, \dot{z}_e, t) \tag{8}$$

In addition, the desired roll and the desired pitch in attitude $\eta_d = \begin{bmatrix} \phi_d & \theta_d & \psi_d \end{bmatrix}^T$ are calculated by the attitude calculation modular (ACM):

$$\eta_d = g_{\eta d}(x_e, y_e, U_1, t) \tag{9}$$

and ψ_d is usually given directly by the reference motion trajectory. In Section 4.3, the attitude control in the attitude loop is obtained by using a sliding mode controller AL-SMC, and the rotation moment solution of attitude control can be obtained by formula (6):

$$U_\eta = f_\eta(\eta_e, \dot{\eta}_e, t) \tag{10}$$

Thus, the torque control components U_2, U_3 and U_4 can be obtained. The problem we try to tackle in this work is to

design a continuous control law u using only to measurable system output ξ and ω such that the error of position and attitude converge to zero in presence of the disturbances. In order to achieve the high precision position and attitude tracking result, a close-loop control strategy is necessary.

III. SYSTEM DESIGN

In this section, a system control scheme is proposed, which provides the tracking controllers and some low-altitude control strategies. Different from the landing and take-off motions of fix-wing UAVs, multi-rotor UAVs have two characteristics: one is that their motions are in a vertical direction relative to the ground, and another is the attitude components pitch and roll tries to maintain zeros. However, the external disturbances and faulty operations often break these rules. A robust control scheme and close-to-ground (CG) planning modules have to be constructed for multi-rotor UAVs flying close to the ground.

A. SYSTEM CONTROL SCHEME

Figure 2 shows the integrated control scheme for UAVs with CG planners. It mainly includes two parts. The 1st part is the system integrated controller, which includes ACM, ATCGP, ALCGP, PL-SMC and AL-SMC. The 2nd part includes the reference trajectories (DT), angular velocity calculation (AVC), UAV and the output feedback of the system. The measurable outputs of UAV include the position perceived by GPS positioning device and altimeter, and the attitude angles and angular velocities perceived by gyroscope. More specifically, ATCGP and ALCGP are deployed to plan the normal flight attitude and the low flight altitude. ACM is an attitude calculation module. PL-SMC and AL-SMC are sliding mode controllers to attenuate the altitude and attitude errors of the UAV's respectively.

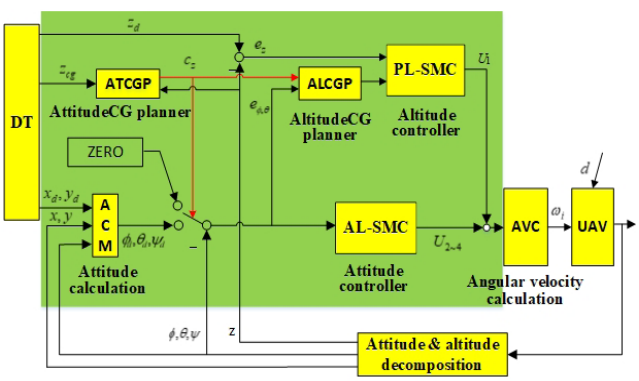

FIGURE 2. Integrated control scheme for UAV with CG planners.

In general, the flight of UAV is classified as high-altitude flight and near-ground flight. According to the magnitude of position deviation, ACM first performs the calculation to obtain the desired attitude. Furthermore, ATCGP determines whether UAV is in the near-ground flight. If so, $c_z = 1$ and the desired values of roll and pitch will be set zero. In addition, if the roll and pitch deviations exceed the admissible upper limits at the same time, ALCGP will increase the attitude adjustment time of the system by increasing the desired altitude. Finally, PL-SMC and AL-SMC derive the control values of the altitude and the attitude respectively based on the sliding mode method.

For the first time, the scheme considers the near-ground threshold distance to play a key role in preventing and reducing rolling overturning of autonomous UAVs. The disadvantage of this method is that UAV may not be able to move rapidly at high speed along the ground in windy weather. However, this characteristic is more in line with the actual safety flight requirements to ensuring the safety of equipment, reducing the possibility of accidents so as to reduce property losses.

B. CG PLANNERS

Unlike the flight control under ideal flight weather conditions, the near-ground flight control under the influence of external wind disturbance is random and complex, and misoperation often occurs. The traditional single attitude and position control mode cannot meet the current control requirements. Instead, this paper considers more factors and parameters such as magnitude of wind velocity, the attitude and angular velocities near-ground distance.

1) ATCGP

In this section, an ATCGP is defined as:

$$c_z = (1 + sign(z_{cg} - z))/2 \tag{11}$$

where z_{cg} is a set minimum altitude of hexacopter, called near-ground threshold distance, so as not to triggered near-ground control. Thus, the output signal $c_z = 1$ denotes the hexacopter is at the low altitude flight.

The desired attitude will be set to zero, shown in the following equation, to avoid collision between UAV and ground obstacles due to large angle adjustment or external disturbances:

$$\eta'_d = \eta_d(1 - c_z)$$

2) ALCGP

A compensation value of the UAV's desired altitude is calculated as:

$$\Delta_h = k_z||e_{\eta-\phi\theta}|| \tag{12}$$

where k_z is the altitude compensation coefficient, and $e_{\eta-\phi\theta}$ is the 2-norm of attitude error e_η in ϕ and θ. Thus, the desired altitude is adjusted by using (13) and the overall lift will increase under the compensation function:

$$z_d = z_d + c_z \cdot \Delta_h \tag{13}$$

Unfortunately, the disturbance force is not easy to be calculated for UAVs with different mass and size profile, as well as the random wind speed and direction. Furthermore, the disturbance magnitude and direction are not easy to be measured

by sensors. Therefore, a robust sliding mode control method is used to solve the problems.

IV. TRAJECTORY TRACKING CONTROL

This section presents the main procedures of position tracking controllers used for handling disturbances existed in the hexacopter to achieve highly precise trajectory tracking. To reduce the tracking error and improve the robustness of the system, sliding-mode control method is used in the altitude tracking controller and attitude tracking controller.

A. PL-SMC DESIGN

In this section, we consider the position loop used for attenuating the tracking position error $\xi_e = [x_e \;\; y_e \;\; z_e]^T$. The deviation between the measured and the desired positions is reduced by a sliding-mode controller PL-SMC. Substituting the position error ξ_e into (5) and neglecting the environmental disturbance d_ξ temporarily, we get:

$$\ddot{\xi}_e = A_\xi U_1 + B_\xi \tag{14}$$

Differentiating (7) to have the velocity tracking error $\dot{\xi}_e$. We express the altitude sliding manifold of hexacopter as:

$$\sigma_z = k_1^z z_e + k_2^z \dot{z}_e \tag{15}$$

where k_1^z, k_2^z are constant control parameters.

The system controller is non-singular. The system remains on the manifold defined by $\sigma_z = 0$, and has the error dynamics $k_1^z \dot{\xi}_e + k_2^z \ddot{\xi}_e = 0$. Substituting Equation (14) into this altitude error dynamics to have the equivalent control:

$$U_1^{eq} = -(1/k_2^z) A_\xi^{-1} (k_1^z \dot{z}_e + k_2^z B_\xi) \tag{16}$$

where U_1^{eq} can be seen as the continuous control law. It would keep the altitude in the absence of unknown disturbances when the system dynamics are exactly known.

As the real system dynamics may exist disturbances, the dynamics (14) can be rewritten as:

$$\ddot{\xi}_e = A_\xi (U_1 + d_\xi) + B_\xi \tag{17}$$

where d_ξ is the environmental disturbance. To drive the system dynamics and keep the system state on the surface $\sigma_z = 0$, we give a new feedback continuous control law as

$$U_1 = U_1^{eq} - \lambda_z \cdot sat(\sigma_z) \tag{18}$$

where λ_z is a positive constant and $sat(\cdot)$ is a continuous saturation function defined as:

$$sat(\sigma) = \begin{cases} -1 & \sigma \le -\delta \\ \sigma/\delta \; |\sigma| < \delta, & \delta > 0 \\ 1 & \sigma \ge \delta \end{cases} \tag{19}$$

where δ denotes the maximum of the variable σ and the function $sat(\sigma)$ is used to smooth out the control discontinuity around zero to reduce undesired chattering caused by imperfection switching of the discontinuous term in the sliding mode control system. A small σ may prevent chattering but increase the tracking error, whereas a large σ may increase chattering and decrease the tracking error. The goal is to achieve a good trade-off between tracking performance and input chattering.

The corresponding control law from (16) becomes:

$$U_1 = -(1/k_2^z) A_\xi^{-1} (k_1^z \dot{z}_e + k_2^z B_\xi) - \lambda_z \cdot sat(\sigma_z) \tag{20}$$

Theorem 1: Considering the dynamics (5) and (6). If a switching function is defined as (15) and environmental disturbance satisfies $d_{\max} \le \lambda_z$, the lift force (20) can reduce the tracking altitude error to zero asymptotically.

Proof: Consider the Lyapunov candidate function:

$$V_z = \frac{1}{2} \sigma_z^T \sigma_z$$

Differentiating V_z with respect to time, we can obtain that:

$$\dot{V}_z = \sigma_z^T \dot{\sigma}_z = \sigma_z^T [k_1^z \dot{z}_e + k_2^z \ddot{z}_e]$$

Substituting (13) into the above equation yields:

$$\dot{V}_z = \sigma_z^T \{k_1^z \dot{z}_e + k_2^z [A_\xi (U_1 + d_\xi) + B_\xi]\}$$

Substitute the control law (15), then $\dot{V}$ can be simplified as:

$$\dot{V}_z = k_2^z \sigma_z^T A_\xi [d_z - \lambda_z \cdot sat(\sigma_z)]$$

where A_ξ is a positive definite coefficient vector, and let $0 \le \rho_z \le \min \; \{k_2^z A_\xi\}$, so we have:

$$\dot{V}_z \le \sigma_z^T \rho_z [d_z - \lambda_z \cdot sat(\sigma_z)] \tag{21}$$

To make (16) negative semi-definite, we will discuss the following two cases respectively. Consider the elements of the vectors σ_z and d_z, if $\sigma_z \ge 0$, then $\sigma_z^T \ge 0$ and $sat(\sigma_z) \ge 0$, so the condition is $d_z \le \lambda_z \cdot sat(\sigma_z) \le \lambda_z$. Otherwise, if $\sigma_z \le 0$, then $\sigma_z^T \le 0$ and $sat(\sigma_z) \le 0$, so the condition is $d_z \ge \lambda_z \cdot sat(\sigma_z) \ge -\lambda_z$. Thus, the system stable condition can be written as $|d_z| \le \lambda_z$.

Furthermore, the upper bound of disturbance is expressed as $d_{z\max}$. Then, whenever σ_z is positive or negative, only if condition $d_{z\max} \le \lambda_z$ is satisfied, there must be $\dot{V}_z \le 0$. The tracking altitude error z_e moves along the sliding manifold to zero. Thus, the altitude of the tracking hexacopter is equal to the desired altitude. Consequently, the altitude closed-loop system is asymptotically stable.□

B. DESIRED ATTITUDE CALCULATION

It has been mentioned that the tracking position error can be translated to the tracking altitude error z_e and the rotational angular error η_e shown in (7). z_e has been discussed and converged to zero under the controller PL-SMC, and the desired attitude $\eta_d = \begin{bmatrix} \phi_d & \theta_d & \psi_d \end{bmatrix}^T$ can also be calculated by the calculation ACM. According to (14), the desired roll and desired pitch angle can be deduced as the form:

$$g_{\eta d} : \begin{cases} \phi_d = \arcsin\left(\dfrac{m(\ddot{x}_e s_\psi - \ddot{y}_e c_\psi)}{U_1}\right) \\ \theta_d = \arcsin\left(\dfrac{m(\ddot{x}_e c_\psi + \ddot{y}_e s_\psi)}{U_1 c_\phi}\right) \end{cases} \tag{22}$$

where U_1 is the lift force shown in (20). In addition, the desired yaw ψ_d is usually decided by the reference motion trajectory which expressed as:

$$\psi_d = h(x_e, y_e, t) \tag{23}$$

The function $h(\cdot)$ gives the heading angle ahead to the target according to the flight trajectory, and the desired attitude η_d will be used in the following procedure of AL-SMC design of the attitude loop.

C. AL-SMC DESIGN

In this section, we consider the attitude loop used for attenuating the tracking attitude error $\eta_e = [\,\phi_e \;\; \theta_e \;\; \psi_e\,]^T$. The deviation of the measured attitude and the desired attitude calculated by the ACM is reduced by a sliding-mode controller AL-SMC. Substituting the error η_e into (6) and neglecting the environmental disturbance d_η, we get:

$$\ddot{\eta}_e = A_\eta U_\eta \tag{24}$$

Differentiating (7) to have the angular velocity tracking error $\dot{\eta}_e$. Considering the switching function, the attitude sliding manifold of hexacopter becomes:

$$\sigma_\eta = k_1^\eta \eta_e + k_2^\eta \dot{\eta}_e \tag{25}$$

where k_1^η, k_2^η are constant control parameters.

The system controller is non-singular. The system remains on the manifold defined by $\sigma_\eta = 0$, and has the error dynamics $k_1^\eta \dot{\eta}_e + k_2^\eta \ddot{\eta}_e = 0$. Substituting Equation (24) into this attitude error dynamics to have the equivalent control:

$$U_\eta^{eq} = -(k_1^\eta / k_2^z) A_\eta^{-1} \dot{\eta}_e \tag{26}$$

where U_η^{eq} can be seen as the continuous control law that would keep the trajectories on the surface in the absence of unknown disturbances when the system dynamics are exactly known. Considering the real system dynamics, the dynamics (24) can be rewritten with environmental disturbance d_η as:

$$\ddot{\eta}_e = A_\eta (U_\eta + d_\eta) \tag{27}$$

To drive the system dynamics to the surface $\sigma_\eta = 0$ and keep the system state on it, we give a new feedback continuous control law below:

$$U_\eta = U_\eta^{eq} - \lambda_\eta \cdot sat(\sigma_\eta) \tag{28}$$

where λ_η is a positive constant, and the function $sat(\cdot)$ is used to reduce undesired chattering caused by imperfections of the switching of the discontinuous term in the sliding mode control system. Thus, the corresponding control law obtained can be given by:

$$U_\eta = -(k_1^\eta / k_2^z) A_\eta^{-1} \dot{\eta}_e - \lambda_\eta \cdot sat(\sigma_\eta) \tag{29}$$

Theorem 2: Consider the hexacopter dynamics in (5) and (6). If the switching function is defined as (25) and environmental disturbance satisfies $d_{\eta\max} \le \lambda_\eta$, the control input moment designed as (29) can render the origin of the tracking attitude error system asymptotically.

Proof: Consider the Lyapunov candidate function:

$$V_\eta = \frac{1}{2}\sigma_\eta^T \sigma_\eta$$

Differentiating V_η with respect to time, we can obtain that:

$$\dot{V}_\eta = \sigma_\eta^T \dot{\sigma}_\eta = \sigma_\eta^T [k_1^\eta \dot{\eta}_e + k_2^\eta \ddot{\eta}_e]$$

Substituting (27) and (29) into the above equation to have:

$$\dot{V}_\eta = k_2^\eta \sigma_\eta^T A_\eta [d_\eta - \lambda_\eta \cdot sat(\sigma_\eta)]$$

where d_η and σ_η are column vectors with three elements, and λ_η is a positive constant. To deduce the system stable conditions, we define $d_{\phi,\theta,\psi}$ and $\sigma_{\phi,\theta,\psi}$ to be their elements of the vectors in their orientations. Since A_η are positive definite matrix, we let $0 \le \rho_\eta \le \min\ \{k_2^\eta A_\eta\}$ so that:

$$\dot{V}_\eta \le \sigma_\eta^T \rho_\eta [d_\eta - \lambda_\eta \cdot sat(\sigma_\eta)] \tag{30}$$

To make (30) negative semi-definite, we consider the elements of the vectors σ_η and d_η. if $\sigma_{\phi,\theta,\psi} \ge 0$, then $\sigma_{\phi,\theta,\psi}^T \ge 0$ and $sat(\sigma_{\phi,\theta,\psi}) \ge 0$. Therefore, the condition is $d_{\phi,\theta,\psi} \le \lambda_\eta \cdot sat(\sigma_{\phi,\theta,\psi}) \le \lambda_\eta$. Otherwise, if $\sigma_{\phi,\theta,\psi} \le 0$, then $\sigma_{\phi,\theta,\psi}^T \le 0$ and $sat(\sigma_{\phi,\theta,\psi}) \le 0$. Therefore, the condition is $d_{\phi,\theta,\psi} \ge \lambda_\eta \cdot sat(\sigma_{\phi,\theta,\psi}) \ge -\lambda_\eta$. Thus, the system stable condition can be written as $|d_{\phi,\theta,\psi}| \le \lambda_\eta$.

Furthermore, the upper bound of disturbance is expressed as $d_{\eta\max}$, and $|d_{\phi,\theta,\psi}| \le ||d_\eta||_2$. Then, whenever the elements of σ_η is positive or negative, only if condition $d_{\eta\max} \le \lambda_z$ is satisfied, there must be $\dot{V}_z \le 0$. The tracking attitude error η_e moves along the sliding manifold to zero. Thus, the attitude of the tracking hexacopter is equal to the desired attitude. Consequently, the attitude closed-loop system is asymptotically stable.□

V. SIMULATION AND EXPERIMENTS

In this section, the proposed control scheme is tested on simulation and experiment platforms of an autonomous UAV with 6 rotors, including autonomous take-off and landing cases, as well as low-altitude control without collision. It is assumed that the altitude is measured by barometric altimeter, the position information is determined by GPS and attitude information is measured by IMU respectively. In addition, the disturbances simultaneously affect roll, pitch, yaw, and altitude dynamics. Table 1 lists the hexacopter parameters.

1) DESCRIPTION OF TIME-VARYING DISTURBANCES

It is well-known that the disturbance torques caused by the wind field is proportional to the wind speed. Therefore, without loss of generality, it is assumed that four different random disturbance torques act on the altitude and attitude channels $\left[\,z \;\; \phi \;\; \theta \;\; \psi\,\right]$ separately. In our simulation, the disturbances are expressed by time-varying functions which include sinusoidal function items with the amplitude range $[1.5, 8](Nm)$ and the frequency range $[0.02\pi, 2.5\pi](rad/s)$ respectively. Figure 3 shows the time-varying disturbance torques.

TABLE 1. Hexacopter parameters used in simulation.

Symbol	Quantity	Numerical value
m	mass of platform	5.2 kg
l	length of arm	0.48 m
I_x	moment of inertia around x-axis	5.6×10^{-3} kg·m^2
I_y	moment of inertia around y-axis	5.6×10^{-3} kg·m^2
I_z	moment of inertia around z-axis	9.1×10^{-3} kg·m^2
C_Q	propeller thrust constant	1.126×10^{-4}
C_T	propeller torque constant	2.365×10^{-5}
r	propeller radius	0.21 m
ρ	air density	1.2 kg/m^3
g	acceleration of gravity	9.81 m/s^2
z_{cg}	near-ground threshold distance	2 m

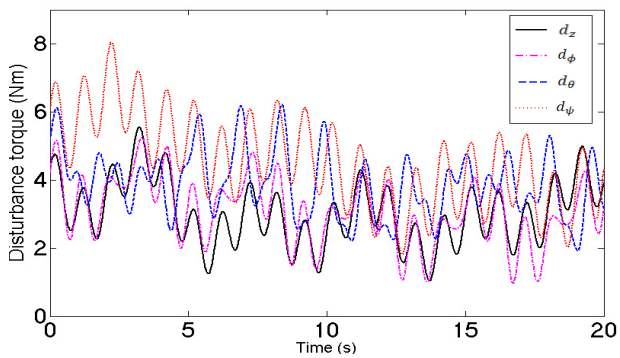

FIGURE 3. Demonstration of the time-varying disturbance torques.

For UAVs, the real-world disturbances are wind force or misoperations, which can be described as the disturbances of control torque. Furthermore, the type of wind disturbance in existed literatures mainly includes constant and time-varying disturbance, and the time-varying disturbance is difficult to be simulated by an accurate mathematical model. However, any form of signal can be decomposed into the superposition of sinusoidal signals with different frequencies. Thus we selected sinusoidal signals as the disturbances whose magnitude can be proportional to the magnitude of the real-world disturbances.

2) CASE 1 (AUTONOMOUS TAKE-OFF TEST WITH NEAR-GROUND CONTROL SCHEME)

In practice, UAVs may tilt at low altitude. In this case, it is assumed that the trajectory of hexacopter is not vertical to the ground at initial take-off phase, and the desired roll is 32°, desired pitch is 9.5° and desired yaw is 10° calculated by only ACM respectively, shown by the dotted line when t < 1.5s in Figure 4. To demonstrate the improved performance of the proposed low-altitude control scheme, the planner ATCGP reset the initial values of the desired attitude to zero, shown by the solid line when t < 1.5s. The altitude and attitude stabilization control in the presence of disturbances are involved when the altitude is less than the near-ground threshold distance $z_{cg} = 2$m.

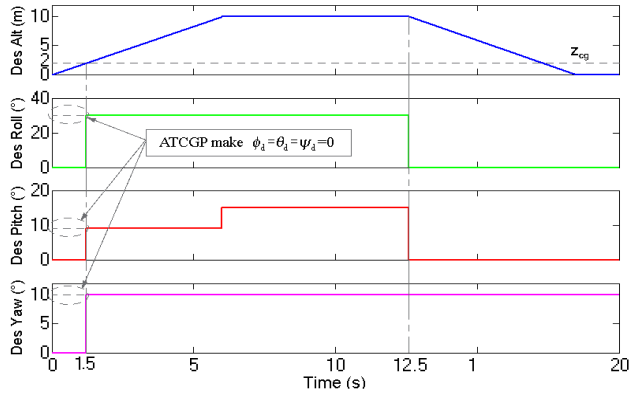

FIGURE 4. Desired altitude and desired attitude, and the values of attitude calculated by ACM are reset zero by ATCGP at the time-period (t < 1.5s).

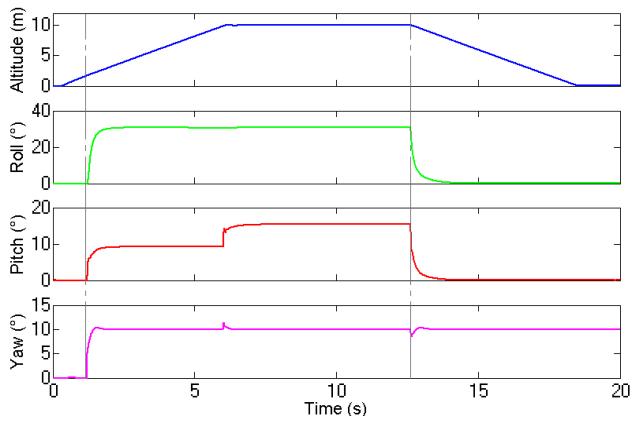

FIGURE 5. Output altitude and attitude curves in Case 1 under near-ground control scheme.

Figures 5 shows the response curves of the altitude and attitude angles of hexacopter during its flight. As can be seen that the output roll and pitch angles maintain zeros at the initial take-off stage and then follow the reference inputs. Thus, the improved near-ground scheme is conducive to avoiding overturning risk due to the big roll and pitch angles from misoperations or external disturbances. In addition, by comparing the output and input curves of the system, it is verified that the proposed position-loop sliding mode controller PL-SMC and attitude-loop sliding mode controller AL-SMC can realize the trajectory tracking control of UAV.

Figure 6 shows the tracking errors in altitude and attitude. In this case, the desired altitude varied continuously, and the output error in altitude adjusted by the PL-SMC controller is very small and nearly negligible. In addition, the proposed AL-SMC controller uses PD sliding manifold and saturation method to reduce the phenomenon which results in a clearly improved performance of the attitude control in the presence of disturbances. The time convergence to the steady state of attitude feedback in these controllers is about 1.5 seconds (shown at time t = 1.5s, 5.2s, 12.5s in Figure 5–6). The error curves results revealed that the proposed PL-SMC and

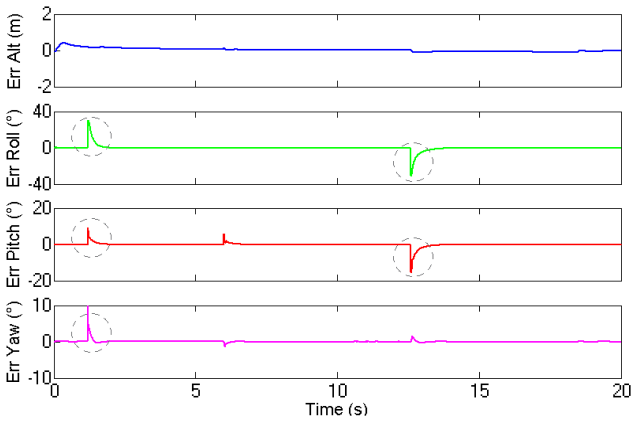

FIGURE 6. Altitude and attitude errors under PL-SMC and AL-SMC.

AL-SMC presented good performance for trajectory tracking and also robustness to external disturbances.

3) CASE 2 (AUTONOMOUS LANDING TEST WITH NEAR-GROUND CONTROL SCHEME)

In this case, we tested a landing flight at low altitude by using proportion integration differentiation (PID), fuzzy logic control (FLC) and sliding mode control (SMC) respectively. The hexacopter needs to adjust its landing position during descent, shown in Figure 7 at t > 5s. When the hexacopter descended to the near-ground threshold distance at 11.5s, the desired roll, pitch and yaw calculated by ACM were still not zero. This is because the hexacopter has not reached the top of the target point. However, at the later flight stages (t ⩾ 11.5s), the planner ALCGP increased the desired altitude from 2m to 5m, which increased the position adjustment time and space. Then the hexacopter flied flat to the target point for hovering and landing.

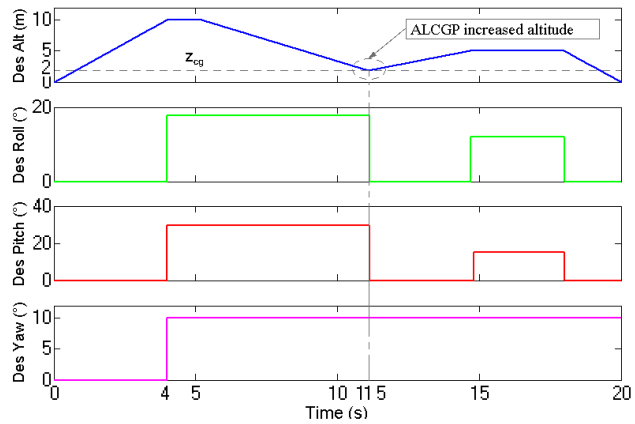

FIGURE 7. Desired altitude and attitude from ACM, and the values of altitude is increased by ALCGP at the time t = 11.5s.

Similar to the case 1, the integrated control scheme was used in this flight test, and the sliding mode controllers PL-SMC and AL-SMC were used to attenuate the tracking errors. For comparison, we also simulated the performance of conventional PID and FLC controllers, prescribing the same flight conditions. Comparing the simulation results (Figures 8(a), (b), (c)), it can be seen that the sliding-mode based output feedback rapidly tracks the desired state without any oscillations or steady state errors.

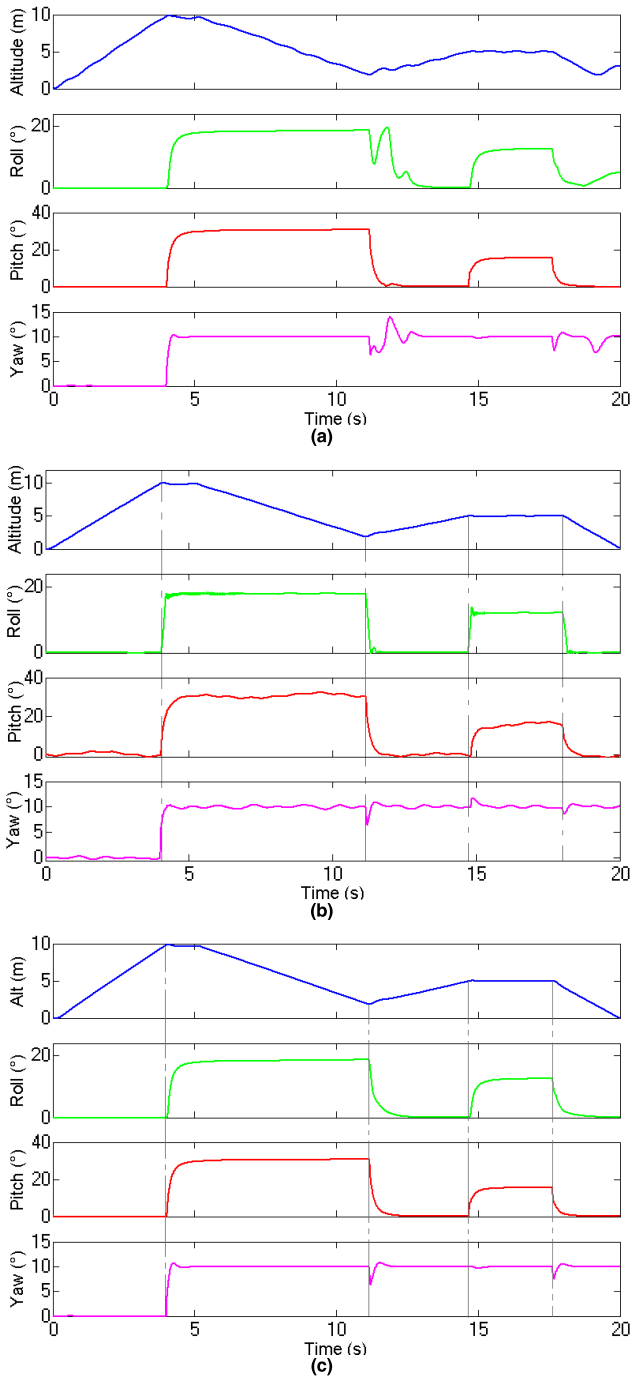

FIGURE 8. Comparison of output altitude and attitude angle performance. (a) Altitude and attitude angles by conventional PID method. (b) Altitude and attitude angles by FLC method. (c) Altitude and attitude angles by proposed integrated method.

For PID based attitude, there was a certain fluctuation of amplitude throughout the flight. At the time period 11s < t < 13s, there were large fluctuations. The hexacopter reached about 13° for roll and 2° for pitch and 5.2° for yaw angles (Figure 8(a)). For FLC based attitude, the violent amplitude fluctuation is eliminated, but there is still small fluctuation. For AL-SMC, the corresponding values are nearly zero for roll and pitch and 2.8° for yaw.

As can be seen in Figure 9(a), the more obvious errors can be classified into two categories according to their sources: Errors caused by Sudden Change of Desired values (Err_SCD) and Errors caused by the External Disturbances (Err_ED). In Figure 9(b), (c), Err_ED are well suppressed and almost eliminated. However, there are still small error fluctuation in Figure 9(c). It can be seen that the control performance is improved by the proposed sliding mode controller compared with the PID controller and the FLC controller. In addition, Figure 9(c) shows that the sliding-mode based tracking error of pitch angle decreases rapidly with the adjustment time $t_s < 0.5$s.

4) EXPERIMENTAL RESULTS

In this case, we have also tested the proposed control scheme on a 6-rotor UAV, DJI M600 Pro, which was used as the autopilot of the hexacopter. To evaluate the stability and robustness of the proposed integrated control scheme, the trajectory tracking control experiments were carried out. M600 Pro is equipped with three redundancy A3 flight controllers. It supports multiple DJI platforms and third-party hardware and software expansion. In order to test our control scheme in real operating conditions, our experiments are run in outdoor environment with wind velocity 1.6-3.3 m/s. After the hexacopter takes off, the landing gear will flatten to both sides shown in Figure 10.

The experiments mainly test the control effect of the proposed integrated control method on the trajectory tracking of the hexacopter. In general, the orientation of the hexacopter is decided by the location of the target detected by the camera. Consequently, yaw is set to a constant in the following experiments and is not shown in result Figures. The experimental curves of the altitude, roll and pitch angles are plotted in Figures 11.

FLC and SMC control methods were used to carry out the flight tests which lasted 60 seconds, respectively. After the hexacopter took off, it stop for a few seconds, then rose vertically to 6 meters, and flied forward. The altitude curves showed that the planner ATCGP set the values of the attitude to zero when the altitude was decreased to 2 meters at t = 28s, then the planner ALCGP increased the altitude back to 6 meters, and the hexacopter flied to the destination and landed vertically.

Comparing Figure 11(a) and (b), both results show that the roll and pitch angles fluctuated greatly when the attitude was adjusting, and we can see that the reduction of the angle fluctuation is close to 40%. However, the roll and pitch angles are less than 2 degrees during the steady flight.

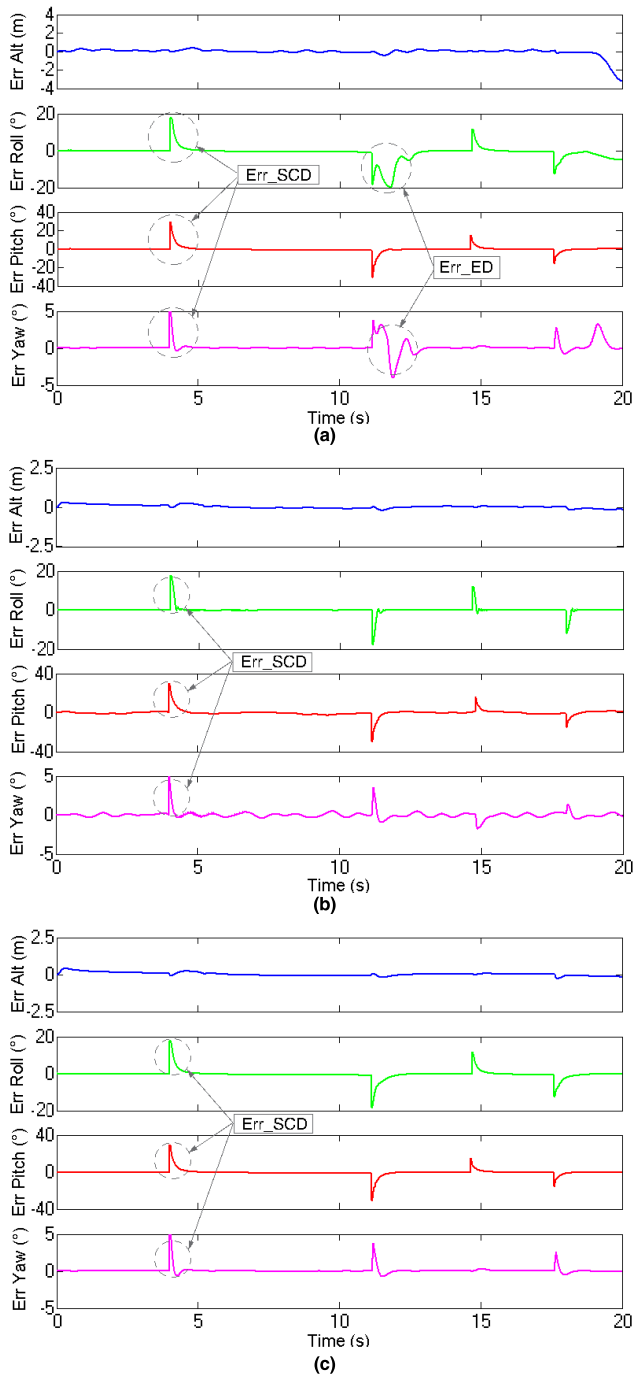

FIGURE 9. Comparison of output altitude error and attitude error. (a) Output errors by PID method. (b) Output errors by FLC method. (c) Output errors by proposed integrated control method.

In addition, the body angular velocities of the hexacopter are recorded and shown in Figure 12. We can see that the roll and pitch angular velocities are very small at most time during the process of the steady flight, and the amplitude also increased slightly corresponding to the real-time attitude adjustments by the proposed feedback controllers (shown at time t = 15s, 25s, 30s, 38s). The roll and pitch angular

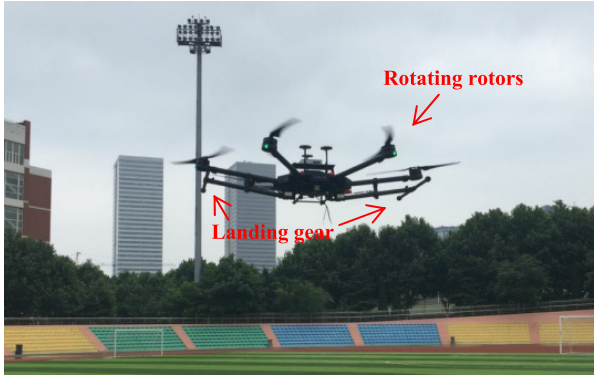

FIGURE 10. Experimental setup of the hexacopter flying on the outdoor playground.

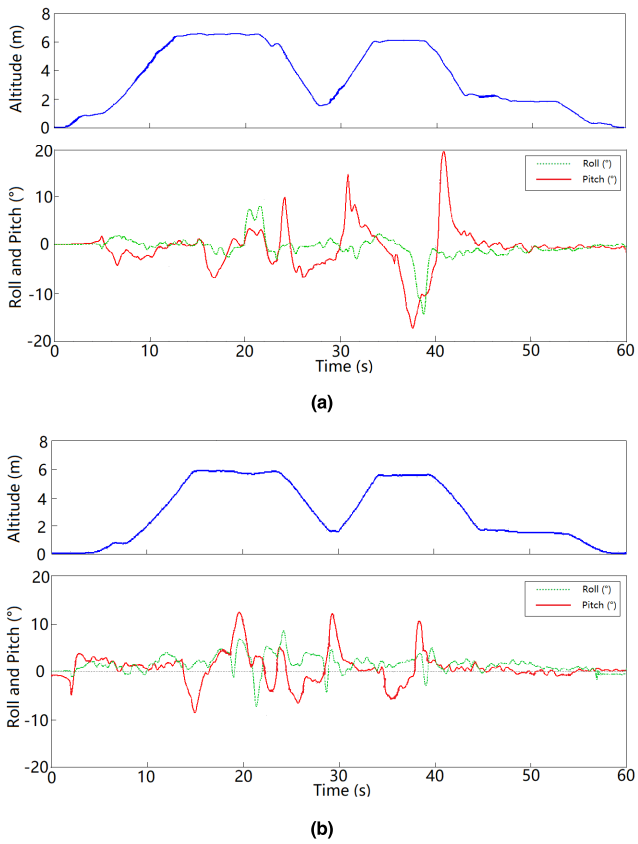

FIGURE 11. Experimental curves of the altitude and attitude. (a) Altitude and roll, pitch angles controlled by FLC method. (b) Altitude and roll, pitch angles controlled by SMC method.

velocities controlled by FLC method are less than 2 rad/s, and the roll and pitch angular velocities controlled by SMC method are less than 1 rad/s. Furthermore, the experimental results are affected by the natural factors, but the controllers are able to quickly alter thrust to counteract the external disturbances and the stability and the convergence of the proposed control laws are proved, which fully reflects the advantages of our planners and integrated control strategy for low altitude flight of UAVs.

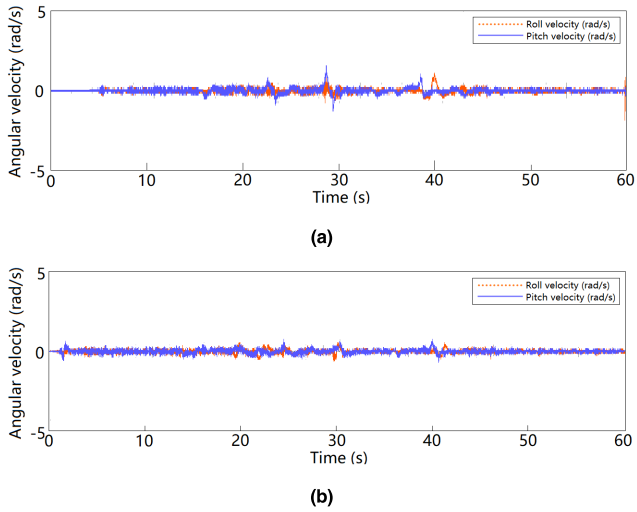

FIGURE 12. Experimental curves of the angular velocities. (a) Roll and pitch angular velocities controlled by FLC method. (b) Roll and pitch angular velocities controlled by SMC method.

In general, the root mean square (RMS) errors of position and attitude of the experimental results are list in Table 2. As can be seen that the RMS reduction of roll angle and pitch angle is 15.48% and 8.17%, respectively.

TABLE 2. Root-mean-square errors of states. Position errors are in meters-rms and angle errors are in radians-rms.

	$x(m)$	$y(m)$	$z(m)$	$\Phi(rad)$	$\theta(rad)$
FLC	0.0619	0.0552	0.0436	0.0017	0.0042
SMC	0.0528	0.0483	0.0432	0.0014	0.0038

In summary, the simulation and experiment results showed that the tested SMC based approach performed well in the presence of external disturbances, i.e., the proposed integrated control exhibited both a fast response and good tracking performance. Simple PID and FLC did not adapt well to these random disturbances, resulting in relatively large oscillations in altitude, roll, pitch and yaw. The best overall performer was the proposed SMC approaches presented in this study which guaranteed the stability of hexacopter and exhibited a fast response and no chattering.

VI. CONCLUSION

In this paper, we proposed a robust control strategy for UAVs at low altitude flight to achieve good performance of disturbance rejection. A second-order hexacopter dynamics was established and the position tracking was translated to the altitude and the rotational angle tracking problem. Considering near-ground operation of hexacopter, an improved flying altitude planner and an attitude planner were designed respectively to avoid the overturning risk due to the big roll and pitch angles. In addition, the sliding-mode based altitude tracking controller and attitude tracking controller are

designed to reduce the tracking errors and improve the robustness of the system. Taking the flight safety into account, it is recommended that the speed of near-ground flight should not be too high, and the flight altitude threshold can be selected by considering the magnitude of external disturbances and possible control torques of misoperations for a small-size hexacopter.

In our future work, disturbance observer can be developed to estimate the external influence accurately so that the performance can be further improved.

REFERENCES

[1] J. Lee, H. S. Choi, and H. Shim, "Fault tolerant control of hexacopter for actuator faults using time delay control method," *Int. J. Aeronautical Space Sci.*, vol. 17, no. 1, pp. 54–63, 2016.

[2] V. Artale, C. L. R. Milazzo, and A. Ricciardello, "Mathematical modeling of hexacopter," *Appl. Math. Sci.*, vol. 7, no. 97, pp. 4805–4811, 2013.

[3] B. Tian, Y. Ma, and Q. Zong, "A continuous finite-time output feedback control scheme and its application in quadrotor UAVs," *IEEE Access*, vol. 6, pp. 19807–19813, 2018.

[4] D. Invernizzi and M. Lovera, "Trajectory tracking control of thrust-vectoring UAVs," *Automatica*, vol. 95, pp. 180–186, Sep. 2018.

[5] J. C. Zufferey, A. Beyeler, and D. Floreano, "Autonomous flight at low altitude with vision-based collision avoidance and GPS-based path following," in *Proc. IEEE Int. Conf. Robot. Automat.*, Anchorage, AK, USA, May 2010, pp. 3329–3334.

[6] S. A. Emami and A. Rezaeizadeh, "Adaptive model predictive control-based attitude and trajectory tracking of a VTOL aircraft," *IET Control Theory Appl.*, vol. 12, no. 5, pp. 2031–2042, 2018.

[7] E. C. Suicmez and A. T. Kutay, "Attitude and altitude tracking of hexacopter via LQR with integral action," in *Proc. Int. Conf. Unmanned Aircr. Syst.*, Miami, FL, USA, Jun. 2017, pp. 150–159.

[8] P. Poksawat, L. Wang, and A. Mohamed, "Gain scheduled attitude control of fixed-wing UAV with automatic controller tuning," *IEEE Trans. Control Syst. Technol.*, vol. 26, no. 4, pp. 1192–1203, Jul. 2018.

[9] B. Erginer and E. Altuğ, "Design and implementation of a hybrid fuzzy logic controller for a quadrotor VTOL vehicle," *Int. J. Control, Autom. Syst.*, vol. 10, no. 1, pp. 61–70, 2012.

[10] C. Fu, A. Sarabakha, E. Kayacan, C. Wagner, R. John, and J. M. Garibaldi, "Input uncertainty sensitivity enhanced nonsingleton fuzzy logic controllers for long-term navigation of quadrotor UAVs," *IEEE Trans. Mechatronics*, vol. 23, no. 2, pp. 725–734, Apr. 2018.

[11] F. Chen, W. Lei, K. Zhang, G. Tao, and B. Jiang, "A novel nonlinear resilient control for a quadrotor UAV via backstepping control and nonlinear disturbance observer," *Nonlinear Dyn.*, vol. 85, no. 2, pp. 1281–1295, 2016.

[12] S. Yu, X. Yu, B. Shirinzadeh, and Z. Man, "Continuous finite-time control for robotic manipulators with terminal sliding mode," *Automatica*, vol. 41, no. 11, pp. 1957–1964, Nov. 2005.

[13] S. Yu and X. Long, "Finite-time consensus for second-order multi-agent systems with disturbances by integral sliding mode," *Automatica*, vol. 54, pp. 158–165, Apr. 2015.

[14] Y. Chen, S. Yu, Z. Shen, and G. Guo, "Cooperative tracking of vessel trajectories based on curved dynamic coordinates," *Asian J. Control.*, 2018, pp. 1–17. doi: 10.1002/asjc.2002.

[15] F. Callou and G. Foinet, "Method for controlling a multi-rotor rotary-wing drone, with cross wind and accelerometer bias estimation and compensation," U.S. Patent 9 488 978 B2, Aug. 11, 2016.

[16] D. Shi, Z. Wu, and W. Chou, "Generalized extended state observer based high precision attitude control of quadrotor vehicles subject to wind disturbance," *IEEE Access*, vol. 6, pp. 32349–32359, 2018.

[17] G. Perozzi, D. Efimov, J.-M. Biannic, L. Planckaert, and P. Coton, "Wind rejection via quasi-continuous sliding mode technique to control safely a mini drone," in *Proc. 7th Eur. Conf. Aeronaut. Space Sci.*, Milan, Italy, Jul. 2017, pp. 1–16.

[18] E. Kayacan and R. Maslim, "Type-2 fuzzy logic trajectory tracking control of quadrotor VTOL aircraft with elliptic membership functions," *IEEE/ASME Trans. Mechatronics*, vol. 22, no. 1, pp. 339–348, Feb. 2017.

[19] J. Baldeón, J. Escorza, D. Chávez, and O. Camacho, "Control for hexacopters: A sliding mode control and PID comparison," *Rev. Téc. Ing. Univ. Zulia.*, vol. 39, no. 3, 137-144, 2016.

[20] H. L. N. N. Thanh and S. K. Hong, "Quadcopter robust adaptive second order sliding mode control based on PID sliding surface," *IEEE Access*, vol. 6, pp. 66850–66860, 2018.

[21] N. Promkajin and M. Parnichkun, "Development of a robust attitude control for nonidentical rotor quadrotors using sliding mode control," *Int. J. Adv. Robotic Syst.*, vol. 15, no. 1, pp. 1–15, 2018.

[22] H. S. Saini, *System Modeling and Simulation of Hexacopter*. Punjab, India: Punjabi Univ., 2016.

[23] R. Schacht-Rodriguez, G. Ortiz-Torres, C. D. Garcia-Beltran, C. M. Astorga-Zaragoza, J. C. Ponsart, and A. J. Perez-Estrada, "Design and development of a UAV experimental platform," *IEEE Latin Amer. Trans.*, vol. 16, no. 5, pp. 1320–1327, May 2016.

[24] R. Niemiec, F. Gandhi, and R. Singh, "Control and performance of a reconfigurable multicopter," *J. Aircr.*, vol. 55, no. 5, pp. 1855–1866, 2014.

[25] D. Lancovs, "Building, verifying and validating a collision avoidance model for unmanned aerial vehicles," in *Proc. Conf. Rel. Statist. Transp. Commun.*, Riga, Latvia, Oct. 2016, pp. 19–22.

[26] A. Joukhadar, M. AlChehabi, C. Stöger, and A. Müller, "Trajectory tracking control of a quadcopter UAV using nonlinear control," in *Proc. Conf. Mechanism, Mach., Robot. Mechatron. Sci.*, Beirut, Lebanon, Oct. 2017, pp. 271–285.

[27] M. A. Lotufo, L. Colangelo, C. Perez-Montenegro, E. Canuto, and C. Novara, "UAV quadrotor attitude control: An ADRC-EMC combined approach," *Control Eng. Pract.*, vol. 84, pp. 13–22, Mar. 2019.

[28] J. Bacik, D. Perdukova, and P. Fedor, "Design of fuzzy controller for hexacopter position control," in *Proc. Conf. 4th Comput. Sci. On-line Conf.*, Zlín, Czech Republic, Apr. 2015, pp. 193–202.

YUQING CHEN received the master's and Ph.D. degrees in control theory and control engineering from the Dalian University of Technology, Dalian, China, in 2003 and 2006, respectively, where he then joined the School of Marine Electrical Engineering, Automation Research Center. From 2014 to 2015, he was a Visiting Research Fellow with the Robotic Lab, Department of Electrical Engineering, City University of New York, USA. He is currently an Associate Professor with the Department of Automation, Dalian University of Technology. His current research interests include nonlinear control theory, intelligent control algorithm and applications in autonomous vessels, unmanned aerial vehicle, autonomous mobile robots, and industrial information networks.

GAOXIANG ZHANG was born in Hunan, China, in 1995. He received the B.S. degree in automatic control from Dalian Maritime University, Dalian, China, where he is currently pursuing the M.S. degree with the School of Control Engineering. His research interests include nonlinear control theory, intelligent control algorithm, applications in unmanned aerial vehicle and autonomous mobile robots, and flight control.

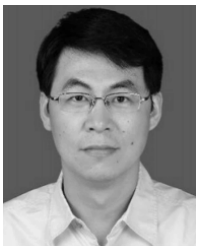

YAN ZHUANG (M'11) received the bachelor's and master's degrees from Northeastern University, Shenyang, China, in 1997 and 2000, respectively, and the Ph.D. degree from the Dalian University of Technology, Dalian, China, in 2004, all in control theory and engineering, where, in 2005, he joined as a Lecturer and became an Associate Professor, in 2007 and he is currently a Professor with the School of Control Science and Engineering. His current research interests include mobile robot 3-D mapping, outdoor scene understanding, 3-D laser-based object recognition, 3-D scene recognition, and reconstruction.

HUOSHENG HU (M'94–SM'01) received the M.Sc. degree in industrial automation from Central South University, Changsha, China, in 1982, and the Ph.D. degree in robotics from the University of Oxford, Oxford, U.K., in 1993. He is currently a Professor with the School of Computer Science and Electronic Engineering, University of Essex, Colchester, U.K., leading the Robotics Research Group. His current research interests include behavior-based robotics, human–robot interaction, service robots, embedded systems, data fusion, learning algorithms, mechatronics, and pervasive computing. He has authored around 500 papers in journals, books, and conferences in these areas. He is a Founding Member of the IEEE Robotics and Automation Society Technical Committee on Networked Robots, and a Fellow of the Institution of Engineering and Technology and the Institute of Measurement and Control. He currently serves as the Editor-in-Chief of the *International Journal of Automation and Computing and Online Robotics Journal*, and the Executive Editor of the *International Journal of Mechatronics and Automation*.